International journal of applied exercise physiology
ISSN: 2322-3537
Vol-14 Issue-01 June 2025

A Corona Recognition Method Utilizing Machine Learning and Perceived Light Color

[1] Sathuluri Beulah, [2] N. Sravani

[1]Assistant Professor, Megha Institute of Engineering & Technology for Women, Ghatkesar.
[2] MCA Student, Megha Institute of Engineering & Technology for Women, Ghatkesar.

Abstract—

Can we detect electric discharge states in gases based on the information on visual images? Using four types of machine learning techniques to extract color, brightness, and shape information features of visible pictures captured by a digital camera, this paper presents a novel approach to building detection models for various phases of corona discharge. Following that, a fresh set of photos is used to evaluate each model. The four distinct machine learning techniques are decision tree (DT), single layer perception (SLP), K-nearest neighbor regression (KNN), and support vector machine (SVM). The prediction results demonstrate that out of the three feature categories, color features perform the best, and out of the four algorithms, KNN performs the best. How to identify the best picture detection regions for improved detection performance is also covered in this article. Results from a variety of cameras and settings are reproduced by our method. The findings show that the color method can still give enough discharge information for practical and economical use in detecting discharge states, even when only the visible light spectrum is recorded from a plasma, since all bands of radiation impact the species that emit visible light.

Index Terms—Color information, discharge state, gray level histogram (GLH), machine learning, red, green, and blue (RGB), visible image.

INTRODUCTION

ELECTRIC discharge is a common component in many types of industrial machinery and is found naturally. Many physical parameters of electrical discharge have been studied by researchers in an effort to understand its features. These parameters include voltage, current, optical spectrum, ultrahigh-frequency electromagnetic waves, number of dis charges, phase angles (for ac discharge), etc. While early studies relied on images (such as the original definition of "corona"), subsequent studies have ignored the relevant optical properties of discharge images. When attempting to figure out discharge geometries, optical measurements definitely perform better than electromagnetic ones. The diagnostic accuracy of conventional identification techniques might be improved by including the optical properties of the discharge picture. Research on discharge images has traditionally relied on qualitative criteria, such as descriptions of morphology and strong or weak light intensity, among others [1]-[5]. Unfortunately, there is less literature on quantitative evaluation. The advancement of computer techniques has led to the widespread use of digital image processing methods for studying discharge characteristics, such as breakdown paths, discharge area, etc., particularly in ultraviolet (UV). These methods can assist with the application of statistical techniques [6], [7] or fractal theory [8]-[10] to tackle complex problems. Gas discharge under these same macroscopic physical conditions is fundamentally random, even if high-speed camera photographs taken on a nanosecond time scale may show certain features of a single discharge. However, a collection of many micro discharges is what the dis charge used in certain industrial applications is actually made of. Statistical analysis of discharge pictures spanning many stochastic processes over an extended period of time is, nevertheless, still much more important than research approaches using high-speed cameras. Referenced as [14]. The color information offered by optical radiation has not been commonly employed in the interpretation of discharge images. In 2000, Russell and Jones [15] proposed the use of chro matic attributes to directly monitor the stability of plasma states. However, at that time, most studies relied on optical-electrical detection techniques, which have a

International journal of applied exercise physiology
ISSN: 2322-3537
Vol-14 Issue-01 June 2025

very wide applicability in terms of general knowledge [15]. It wasn't until 2009 that Koppisetty et al. [16] attempted to connect the color information of the visual pictures to the partial-vacuum breakdown process. The use of color information for arc welding monitoring was demonstrated by Serrano et al. [17] in 2016. Nothing new has happened in the realm of no thermal plasmas. We sought patents for methods that use color information to identify the state of discharge [18]-[20] and studied the differences between corona and surface discharges in terms of color. In 2017, Prasad and Reddy [21], [22] introduced a method for extracting color information from discharge images, which was then converted to brightness metrics to study the relationship with discharge power, which is an important progress. As a whole, research into the geographical distribution of no thermal plasma discharge using color information is a relatively new field.

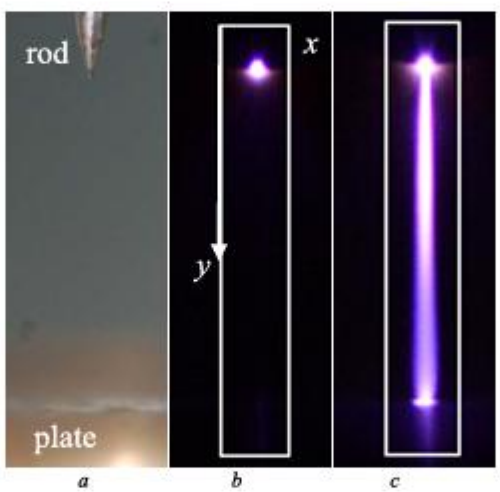

Fig. 1. (a) Electrode configuration and (b) and (c) discharge images,

Thanks to the new high-resolution digital cameras, (a) U = 5.5 kV, (b) U = 6 kV, and the exposure period t = 6s. Machine learning and artificial intelligence studies have come a long way in the last few years. In high-voltage areas, these methods have shown to be quite useful in resolving nonlinear, high-dimensional issues. For instance, prior studies have investigated the use of neural networks and support vector machines to identify patterns in insulator circumstances [23], polyradial phase difference [24]–[26], ultrahigh frequency pattern recognition [27], and fusion plasmas [28], [29]. Being the first to use machine-learning techniques to interpret visual pictures' color information, our study is groundbreaking. In addition to support vector machines (SVM), we have also investigated other methods for analysis such as decision trees (DT), single layer perceptions (SLP), and K-nearest neighbor regression (KNN). Regression challenges requiring supervised learning find extensive use in these techniques. We won't go into the algorithms here, but there are plenty of resources for learning everything about machine learning techniques. Sections [30] through [33]. In order to construct several detection models for distinct corona discharge states, this paper suggests using machine learning techniques to extract visual picture features such as color, brightness, and form. Corona discharge experimental set is presented in the second section. Part three will present the concept of a three-primary-color gray-level histogram (RGB-GLH) for visual pictures and talk about the steps involved in using machine learning algorithms to assess the graphical images' characteristic information. In the fourth section, we report and compare our model's prediction outcomes. At last, we will give you the rundown.

EXPERIMENTAL SETUP

The rod-plate discharge system is shown in Figure 1(a). The rod-plate gap is 8 mm, and the rod diameter is 0.64 mm. A tungsten rod serves as the top electrode and is linked to an alternating current (ac) power source. A copper plate serves as the bottom electrode and is linked to ground via a resistor (R = 50). A 50 Hz frequency is used for the applied ac voltage. The applied voltage is measured using a high-voltage probe (Tektronix P6015A), while the current is measured using the resistor. All of the discharge photographs were captured with a Nikon D800 with the following settings: ISO 2000, 3200, and 5000, with exposure lengths of 2, 4, and 6 seconds, respectively. Alternating voltages produce the classic corona images seen in Fig. 1(b) and (c). Part three.

MACHINE LEARNING

Before we can begin to build detection models for various corona discharge states, we must first prepare our image library using digital camera images. Then, we must choose feature quantities, such as color, brightness, and shape information characteristics of visible images. Lastly, we must apply four types of machine learning algorithms—SVM, KNN, SLP, and DT—and compare their performances. A. Creating an image archive at ten different voltages ranging from zero to six kilovolts, we recorded images of corona discharge: zero, two, three, five, and six kilovolts. The total number of photographs created is 900, which is the result of taking ten shots at 2, 4, and 6 s exposure durations and three different ISOs (2000, 3200, and 5000, respectively) for each voltage. The voltage value, rather than the exposure duration or ISO, is shown on the label of every photograph. According to Figure 1(c), 6 kV is still in the prebreakdown state. B. Information extraction based on characteristics every picture has a lot of pixels. To get enough useful color information from the chosen regions of pixels, x ∈ (0,150), y ∈ (0,950), as shown in Figure 1(b), we used the same area of (m × n =150×950) pixels in all the photographs. Each pixel's color in a color imaging system is represented by an RGB value, which is a combination of the three basic colors. Typically, in computing, an 8-bit representation is used for each primary color, with integer values ranging from 0 to 255. The intensity and brightness of the main color shows are proportional to the value. Therefore, the color information on the connected locations is represented by the retrieved RGB values. The histogram may be used to determine the distribution of R, G, and B values in the chosen region (m × n) by defining a bin for each potential value (256 bins total) and counting the pixels in each bin. After that, we divide our histogram by the entire pixel count to get the frequency of occurrence. As shown in Figure 2 (which corresponds to Figure 1(b)), we will use an RGB-GLH to denote this probability distribution. In Fig. 3, which corresponds to Fig. 1(c), we can see that it enters the prebreakdown stage as the voltage rises. While a rise in voltage causes a noticeable shift in its distribution, calculating an accurate index of this shift is no easy task and requires careful analysis. There are 3 × 256 data points per RGB-GLH in the discharge area.

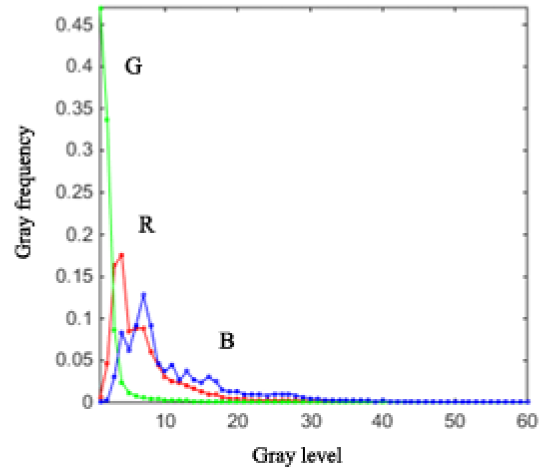

Fig. 2. Three primary color GLH (RGB-GLH), U = 5.5kV.

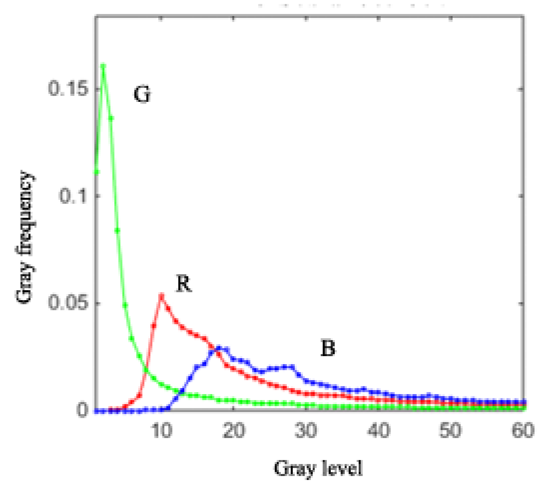

Fig. 3. Three primary color GLH (RGB-GLH), U = 6kV.

Image. Machine learning is useful here since it seems to be difficult to directly study these data points without losing sight of the whole picture. We also investigated the possibility of using the GLH of a monochrome picture as a feature. By using gray level characteristics, we are able to selectively preserve and take into account brightness-related data. There are only 256 points per picture in this category's output feature. Methods for deriving data properties from observable pictures. The four kinds of machine-learning algorithms are SVM, KNN, SLP, and DT algorithms. For data binary classification utilizing supervised learning and kernel approaches, support vector machines (SVMs) are a generalized linear classifier. It is a popular kernel-learning approach

International journal of applied exercise physiology
ISSN: 2322-3537
Vol-14 Issue-01 June 2025

that may be used for nonlinear data classification. Among the many approaches to data mining categorization, the KNN algorithm stands out as particularly straightforward. The basic premise of KNN is that a sample X is given the characteristics of samples in a category if the majority of its k-most near neighbors in the feature space also belong to that category. SLP is an example of a feed-forward artificial neural network that is basic and has just one layer. One way to get close to the discrete function's value is via DT. Following data processing, an induction algorithm generates DTs containing understandable rules. Next, each incoming data piece is categorized by traversing the tree structure in a top-down fashion. In terms of prediction, each of our algorithms would only provide a single class for any given picture. After randomizing the order of the 900 photographs, we divide the dataset into 20 separate folds, with 45 images in each fold. Each time, we set aside a new fold to be evaluated, while the other nineteen are trained using machine learning techniques to extract the RGB-GLH, brightness, or form characteristic. The outcomes of 20 groups' cross-validation are thus obtained. Here are the specifics of the findings. Voltage predictions are made using our trained model. Our model's final assessment score is derived by averaging the twenty RMSE values obtained after 20 iterations of the training and testing procedures. 20 MeanRMSE = we tried out related features utilizing histogram-oriented gradients (HOG) and examined the shape information of the black-and-white picture. For each pixel block, HOG calculates his to grams for gradients in order to ascertain the local form or orientation. We used HOG algorithms on our 150×950 pixel picture with parameters (8, 4, orientation bin size, pixels per cell). For every picture, we obtained a matrix with the following values: (115, 15, 4, 4, 8), which stands for (number of blocks per row, number of blocks per column, number of cells per row, number of cells per column, and number of orientations). A feature vector is created by flattening this.

$$\mathrm{RMSE}(k) = \sqrt{\frac{1}{45}\left(\sum_{j=1}^{45}\left(U_{\mathrm{pre}}^{\mathrm{k}}(j) - U_{\mathrm{lab}}^{k}(j)\right)^2\right)}. \quad (1$$

$$\mathrm{MeanRMSE} = \frac{\sum_{k=1}^{20}\mathrm{RMSE}(k)}{20}. \quad (2)$$

RESULT ANALYSIS

The computational and experimental findings will be presented now. Four detection models are constructed initially. Secondly, we provide a talk on how to choose the best picture detection regions. Lastly, we zero in on the KNN approach that makes use of RGB-GLH data as a feature based on the outcomes of the prior study. Part A: Outcomes from Various Algorithms and Data on Distinct Variables C. ML with Cross-validation in Action Using four distinct ML techniques, we construct several detection models for distinct corona discharge conditions. The outcomes of using various algorithms and varying characteristics are shown in

Table I. The experiment was repeated with the area m × n = 150×950.

	SVM	KNN	SLP	DT
Color	0.692	**0.549**	1.053	0.7
Brightness	0.882	1.044	1.241	0.74
Shape	0.897	0.709	56.85	1.236

When comparing the outcomes of color, brightness, and shape feature information in various methods, the findings demonstrate that the RGB-GLH error is the least. This information is shown in each column of Table I. When color is utilized as a feature, KNN has the fewest error of the four algorithms, as seen in the second row of Table I. Out of the three feature categories, color features seem to be the most effective, and out of the four algorithms, KNN seems to be the most effective. Out of the three types of features, color features capture the most relevant information about the discharge status, which is likely why they outperform brightness features. On the other hand, shape features are high dimensional, so our model may struggle to capture their underlying information without dimensionality reduction techniques. One possible explanation for KNN's superior performance is because it uses a high-dimensional matrix to group pictures into clusters based on their voltage, which means that images with comparable voltages will be grouped together. Similar to how SVM performs, it is effective at handling high-dimensional data by using kernel algorithms to identify hyper planes that divide the data. However, DT may not be able to capture the intricacy of our situation, particularly with regard to

International Journal of applied exercise physiology

ISSN: 2322-3537
Vol-14 Issue-01 June 2025

the shape feature, as it utilizes a single feature point simultaneously for tree node splitting without any modification. Similarly, SLP is insufficient for data fitting since it only includes one layer of hidden units. The KNN approach, which makes use of RGB-GLH data, will be the subject of our attention next. Our training and cross-validation results show that a Mean RMSE of 0.549 is obtained using KNN employing the RGB-GLH information characteristic for x ∈ (0,150) and y ∈ (0,950). To determine the best region to pick, we repeat the procedure five times by changing the vertical length y, for example, x ∈ (0,150), and y ∈ (0,800). Figure 4 displays the discrete points and the trend. We can determine that the inaccuracy is at its lowest when the area is about equal to 150 × 650 from the curve in Figure 4. The fact that the discharge area is not proportional to the voltage is a reasonable explanation for this. Consequently, choosing a big region would reduce the concentration of useful data inside the

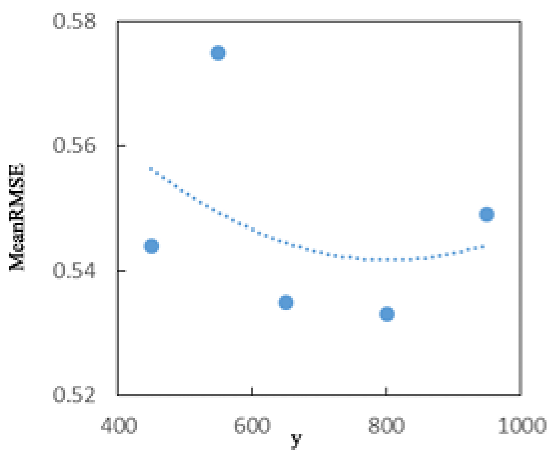

Fig. 4. MeanRMSE of KNN using RGB-GLH of different sizes of regions.

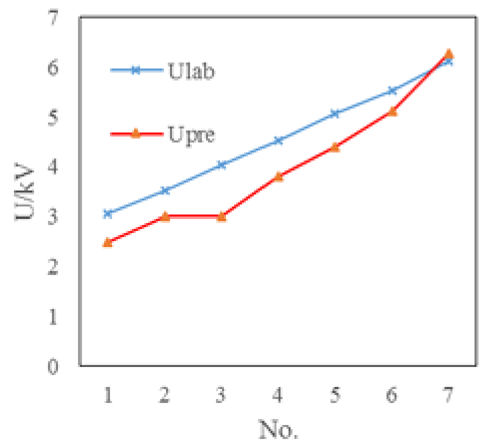

Fig. 5. Predicted voltage (KNN) and labeled voltage for other camera images.

Whereas a smaller region may not provide enough information about changes in discharge data for a dataset with dimensions m×n=150×650. The ideal detection area for our model is 150 × 650, and the MeanRMSE is 0.535. Findings from KNN Models Using RGB-GLH Data from Various Cameras Up until now, we have been using a Nikon D800 camera, which comes with an image size of 7360 × 4912 with ISO rates of 2000, 3200, and 5000. In order to test the model on photographs captured by the Nikon D50, we will be using a 3008 × 2000 image size, 1600 ISO, and an eight-second exposure period. The model was previously trained on images from the Nikon D800. For seven photos, Fig. 5 shows the anticipated voltages Upre and the labeled voltages (measured) Ulab. Our model regularly performs well with the new photoset, averaging a 0.5-kV inaccuracy.

CONCLUSION

Color features outperform the other two qualities in terms of prediction accuracy, while the KNN method outperforms the other three algorithms in terms of accuracy overall.
The model maintains its high level of performance across a variety of cameras and settings. Discharge emits light of many wavelengths, including ultraviolet, visible, and near infrared. While most previous research has focused on ultraviolet light, spectral measurements show that visible light

International journal of applied exercise physiology
ISSN: 2322-3537
Vol-14 Issue-01 June 2025

radiation may be just as intense. Radiation from any spectrum may influence objects that are capable of emitting visible light. This means that our RGB-GLH technique may include discharge status-related information across spectra, allowing us to construct a more accurate model, even if it just employs visible spectrum information. Even if you're not dealing with a corona discharge, you may still use the RGB color information characteristics technique.

REFERENCES

[1]. D. T. Markus and T. S. Lee, "A method of direct corona imaging on a dielectric transparency," IEEE Trans. Ind. Appl., vol. 32, no. 4, pp. 832–836, Jul. 1996.

[2]. Y. Arao, T. Fujii, and M. Yatsuzuka, "Image evaluation of atmospheric corona discharge applied for road tunnel high-velocity electrostatic precipitator," IEEE Trans. Plasma Sci., vol. 33, no. 2, pp. 312–313, Apr. 2005.

[3]. P. H. Ceccato, O. Guaitella, M. Le Gloahec, and A. Rousseau, "Time resolved nanosecond imaging of the propagation of a corona-like plasma discharge in water at positive applied voltage polarity," J. Phys. D: Appl. Phys., vol. 43, no. 17, 2010, Art. no. 175202.

[4]. S. N. Abolmasov, K. Tachibana, and T. Shirafuji, "Mechanisms of pattern formation in dielectric barrier discharges," IEEE Trans. Plasma Sci., vol. 39, no. 11, pp. 2090–2091, Nov. 2011.

[5]. M. Liao, J. Huang, G. Ge, X. Duan, Z. Huang, and J. Zou, "Vacuum arc commutation characteristics of the DC microgrid hybrid circuit breakers," IEEE Trans. Plasma Sci., vol. 45, no. 8, pp. 2172–2178, Aug. 2017.

[6]. D. B. Watson, S. K. Kho, K. A.Samuels, L. Ma, and J. B. Chiu, "Impulse f lashover trajectory in air in nonuniform fields," IEEE Trans. Electr. Insul., vol. 28, no. 2, pp. 200–208, Apr. 1993.

[7]. D. Amarasinghe, U. Sonnadara, M. Berg, and V. Cooray, "Correla tion between brightness and channel currents of electrical discharges," IEEE Trans. Dielectrics Electr. Insul., vol. 14, no. 5, pp. 1154–1160, Oct. 2007.

[8]. J. M. K. MacAlpine, D. H. Qiu, and Z. Y. Li, "An analysis of spark paths in air using 3-dimensional image processing," IEEE Trans. Dielectrics Electr. Insul., vol. 6, no. 3, pp. 331–336, Jun. 1999.

[9]. D. H. Qiu, J. M. K. MacAlpine, and Z. Y. Li, "An incremental analysis of spark paths in air using 3-dimensional image processing," IEEE Trans. Dielectrics Electr. Insul., vol. 7, no. 6, pp. 758–763, Dec. 2000.

[10]. L. Kebbabi and A. Beroual, "Fractal analysis of creeping discharge patterns propagating at solid/liquid interfaces: Influence of the nature and geometry of solid insulators," J. Phys. D: Appl. Phys., vol. 39, no. 1, pp. 177–183, Jan. 2006.

[11]. C. Liu, D. Dobrynin, and A. Fridman, "Uniform and non-uniform modes of nanosecond-pulsed dielectric barrier discharge in atmospheric air: Fast imaging and spectroscopic measurements of electric fields," J. Phys. D: Appl. Phys., vol. 47, no. 25, Jun. 2014, Art. no. 252003.

[12]. B. Pongrác, H. H. Kim, M. Janda, V. Martišovitš, and Z. Machala, "Fast imaging of intermittent electrospraying of water with positive corona discharge," J. Phys. D: Appl. Phys., vol. 47, no. 31, 2014, Art. no. 315202.

[13]. J. M. Palomares, A. Kohut, G. Galbács, R. Engeln, and Z. Geretovszky, "A time-resolved imaging and electrical study on a high current atmospheric pressure spark discharge," J. App. Phys., vol. 118, no. 23, 2015, Art. no. 233305.

[14]. X. Li et al., "Statistical evaluation of AC corona images in long-time scale and characterization of short-gap leader," IEEE Trans. Dielectr. Electr. Insul., vol. 23, no. 1, pp. 165–173, Feb. 2016.

[15]. P. C. Russell and G. R. Jones, "Chromatic monitoring of plasma and plasma systems," Vacuum, vol. 58, pp. 88–99, Aug. 2000.

[16]. K. Koppisetty, M. Serkan, and H. Kirkici, "Image analysis: A tool for optical-emission characterization of partial-vacuum breakdown," IEEE Trans. Plasma Sci., vol. 37, no. 1, pp. 153–158, Jan. 2009.

ISSN: 2322-3537
Vol-14 Issue-01 June 2025

[17]. J. M. Serrano, R. Ruiz-Lombera, J. J. Valdiande, A. Cobo, and J. M. Lopez-Higuera, "Colorimetric analysis for on-line arc-welding diagnostics by means of plasma optical spectroscopy," IEEE Sensors J., vol. 16, no. 10, pp. 3465–3471, May 2016.

[18]. Q. Ye, F. Li, and Y. Hu, "A method of dividing corona discharge stage by visible light image chromaticity processing," CN Patent 106778855 A, Dec. 8, 2016.

[19]. Q. Ye and Z. Guo, "A visible light image RGB recognition method for transmission equipment corona in sunlight environment," CN Patent 107862317 A, Oct. 23, 2017.

[20]. Q. Ye, X. Dong, and Y. Wang, "A method of diagnosing surface discharge based on visible light in sunlight environment," CN Patent 108230408 A, Jan. 18, 2018.

[21]. D. S. Prasad and B. S. Reddy, "Study on corona activity using an image processing approach," IEEE Trans. Ind. Appl., vol. 53, no. 4, pp. 4008–4014, Jul./Aug. 2017.

[22]. D. S. Prasad and B. S. Reddy, "Digital image processing techniques for estimating power released from the corona discharges," IEEE Trans. Dielectr. Electr. Insul., vol. 24, no. 1, pp. 75–82, Feb. 2017.

[23]. V. S. Murthy, K. Tarakanath, D. K. Mohanta, and S. Gupta, "Insula tor condition analysis for overhead distribution lines using combined wavelet support vector machine (SVM)," IEEE Trans. Dielectr. Electr. Insul., vol. 17, no. 1, pp. 89–99, Feb. 2010.

[24]. H. Janani, B. Kordi, and M. J. Jozani, "Classification of simultaneous multiple partial discharge sources based on probabilistic interpretation using a two-step logistic regression algorithm," IEEE Trans. Dielectr. Electr. Insul., vol. 24, no. 1, pp. 54–65, Feb. 2017.

[25]. K. Wang et al., "A new image-oriented feature extraction method for partial discharges," IEEE Trans. Dielectr. Electr. Insul., vol. 22, no. 2, pp. 1015–1024, Apr. 2015.